EPJ Web of Conferences **298**, 01002 (2024) https://doi.org/10.1051/epjconf/202429801002
UCANS-10

Recent status and measurement examples of the compact accelerator-driven neutron facility AISTANS

Koichi Kino[1*], *Takeshi* Fujiwara[1], *Brian E.* O'Rourke[1], and *Nagayasu* Oshima[1]

[1] National Institute of Advanced Industrial Science and Technology (AIST), 305-8568 Tsukuba, Ibaraki, Japan

Abstract. AISTANS, which is optimized for the Bragg-edge imaging, has been utilized for industrial applications. A second beamline was recently constructed and is under preparation for neutron analysis use. The power of the electron beam, which is used for neutron production at a tantalum target, is currently approximately 1 kW and it is planned to be increased. At AISTANS, various sizes of automobile parts have been analysed non-destructively by neutron radiography, computed tomography, and the Bragg-edge method. Recently, other industrial applications such as analysis of lithium-ion batteries using Bragg-edge spectroscopy have been performed. The neutron diffraction method using a newly developed diffractometer is combined for the Bragg-edge analysis.

1 Introduction

AISTANS is a compact accelerator-driven neutron source (CANS) dedicated for industrial applications located at AIST in Tsukuba, Japan [1-3]. It was developed for a non-destructive analysis project aimed at weight reduction of transportation vehicles. The analysis methods are neutron radiography, computed tomography (CT), and Bragg-edge imaging. At AISTANS, an electron linear accelerator and decoupled solid methane moderator, which are suitable for short neutron pulsed-beam production, are used and the design is optimized for Bragg-edge imaging.

In 2021, we succeeded in producing a thermal-cold pulsed neutron beam. Subsequently, various non-destructive analysis of automobile parts was performed under the auspices of the original AISTANS project. From 2023, we are applying AISTANS to other industrial applications like lithium-ion batteries. Furthermore, we developed a neutron diffractometer, which utilizes the short neutron pulse, and the obtained spectra help with the understanding of the Bragg-edge spectra. In this paper, recent developments and the operation status of AISTANS and measurements and data analysis at AISTANS are shown.

* Corresponding author: koichi.kino@aist.go.jp

2 Status of development and operation of AISTANS

AISTANS was initially developed for a beamline optimized for Bragg-edge imaging, which uses a decoupled solid methane moderator (~20 K) and a neutron flight path length for Bragg-edge imaging of around 8 m. The decoupled solid methane moderator is just above a tantalum neutron-production target irradiated by an electron beam from an electron linear accelerator. The size of this moderator is 12 cm (H) × 12 cm (W) ×3 cm (T). Recently a second beamline was constructed. In this beamline, two types of pulsed neutron beam are available, a thermal-cold neutron beam from a coupled solid methane moderator (12 cm (H) × 12 cm (W) ×5 cm (T)) and a pulsed fast neutron beam directly from the neutron production target. The former beam has high intensity from the coupled solid methane moderator and is suitable for neutron radiography and CT. The latter beam is suitable for irradiation of fast neutrons, for example investigation of soft-error by direct irradiation of electronic devices. The second beamline is now operational and will be used in the near future. The measurements shown in this paper were performed at the first beamline.

The electron linear accelerator at AISTANS is currently operated with an electron energy of 37 MeV, repetition rate of 20 Hz, pulse width of 8 μs, and a peak current of approximately 200 mA. The corresponding electron beam power is approximately 1 kW. It is planned to increase the beam power and thus the neutron flux at a measurement sample position, mainly by increasing the repetition rate while paying attention to the electron beam parameters and the heat load to the electron-beam extraction window, the target and surrounding radiation-shielding materials.

3 Imaging examples of automobile parts

Various neutron imaging was performed for automobile parts at AISTANS. Large sized samples (door panel, suspension, etc.), small sized samples (FSSW (Friction Spot Stir Welding) and adhesion samples), and material samples (Carbon steel, TRIP (Transformation-induced plasticity) steels) were imaged. An example of the radiography of an automobile transmission (gearbox) is shown in Fig. 1.

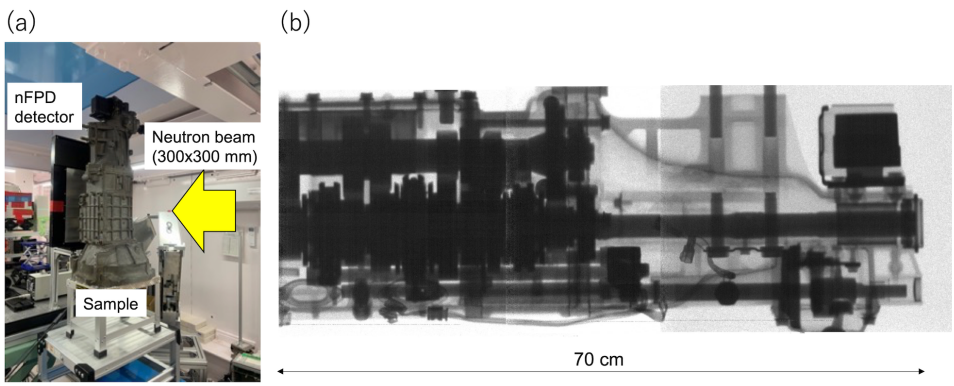

Fig. 1 Neutron radiography of an automobile transmission sample. (a) Photograph of the measurement set-up. (b) Obtained radiography image.

For the purposes of this experiment, a neutron flat-panel detector (nFPD), developed by Fujiwara et al. [4], was employed. The nFPD is comprised of a scintillator, a photodiode, an IGZO thin-film transistor (TFT), and analog front-end circuits for readout purposes. This research utilized a 320 μm thick LiF/ZnS:Ag scintillator sheet (EJ-426HD, Eljen Technology, Ltd., USA) as the neutron converter. The scintillator sheet was directly coupled to a photodiode pixel array equipped with an IGZO TFT readout, tasked with detecting the visible light emitted from the scintillator. The nFPD features a resolution of 1280 × 1550 pixels, with a pixel pitch of 200 μm, and a field of view measuring 25.6 cm × 31.0 cm. Owing to IGZO's high neutron tolerance, this IGZO TFT-based nFPD does not require a fiber-optic plate or any other coupling devices on the surface of the photodiode array. This design facilitates a nearly theoretical spatial resolution of 200 μm. Fig. 1 (a) shows the photograph of the measurement set-up. A 300×300 mm size neutron beam was irradiated on the sample, which is 700 mm in length, at three different areas on the sample. The irradiation time for each picture was 500 seconds. The image obtained by combining all three pictures is shown in Fig. 1 (b). The internal structure can be clearly recognized even within such large sized automobile parts.

4 Development of a diffractometer

The short-pulsed neutron beam available at AISTANS is also useful for neutron diffraction measurement, although it was initially optimized for the Bragg-edge imaging. The resolution of the lattice spacing by the time-of-flight (TOF) method is defined by two elements: (a) the neutron scattering angle resolution and (b) the neutron TOF resolution [5]. At AISTANS, the central scattering angle was set to be 144 °, which is the maximum value in the range of geometrically allowance, to reduce element (a) so that element (b) is dominant. The He-3 position sensitive detector (PSD) at the end of the diffractometers has a sensitive area of 100 × 600 mm and the range of the neutron scattering angle is from 133° to 154°. Therefore, the property of the neutron short pulse is effectively utilized.

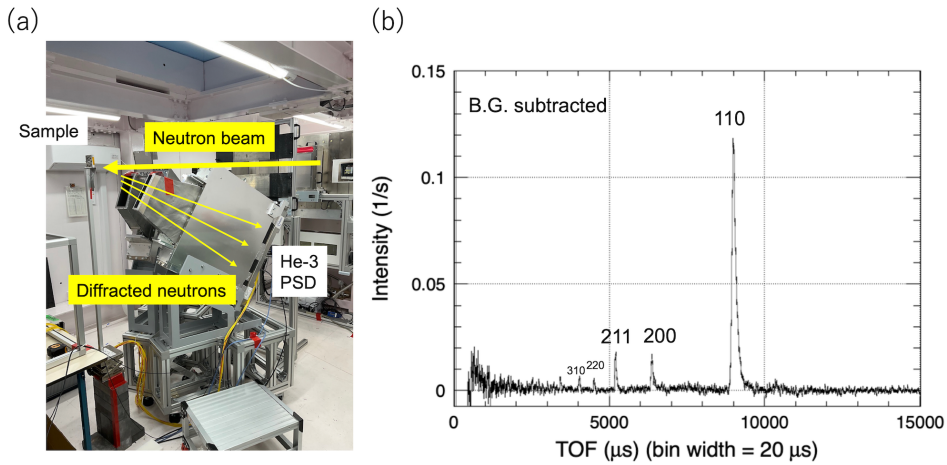

Fig. 2 Neutron diffractometer and an example of diffraction spectrum. (a) Photograph of the diffractometer. (b) Diffraction spectrum obtained by an iron powder sample.

Fig. 2 (a) shows a photograph of the diffractometer. Two identical diffractometers are set symmetrically to the neutron beamline. Fig. 2 (b) shows a measurement spectrum for a BCC (body centered cubic) iron powder sample. The sample amount is 6.1 g, and the measurement time is 5 hours. The background in the spectrum is subtracted. There are many sharp diffractions peaks corresponding to the BCC iron. For example, the width of the 110-reflection peak in FWHM is approximately 1 % and this is dominated by the neutron pulse width [6].

5 Applications to battery

We have applied AISTANS to Bragg-edge imaging of lithium-ion batteries (LIBs). The state of charge can be non-destructively imaged by analysing the Bragg-edge spectrum at each imaging pixel originating from crystalline information of the electrode [7-9]. Quantitative imaging of the battery charge/discharge state was previously performed at J-PARC, which provides short-pulsed neutron beam [7].

Fig. 3 (a) shows the LIB sample. This is a commercial flat plate type LIB for smart phones. The area is 100×45 mm and the thickness is 3 mm.

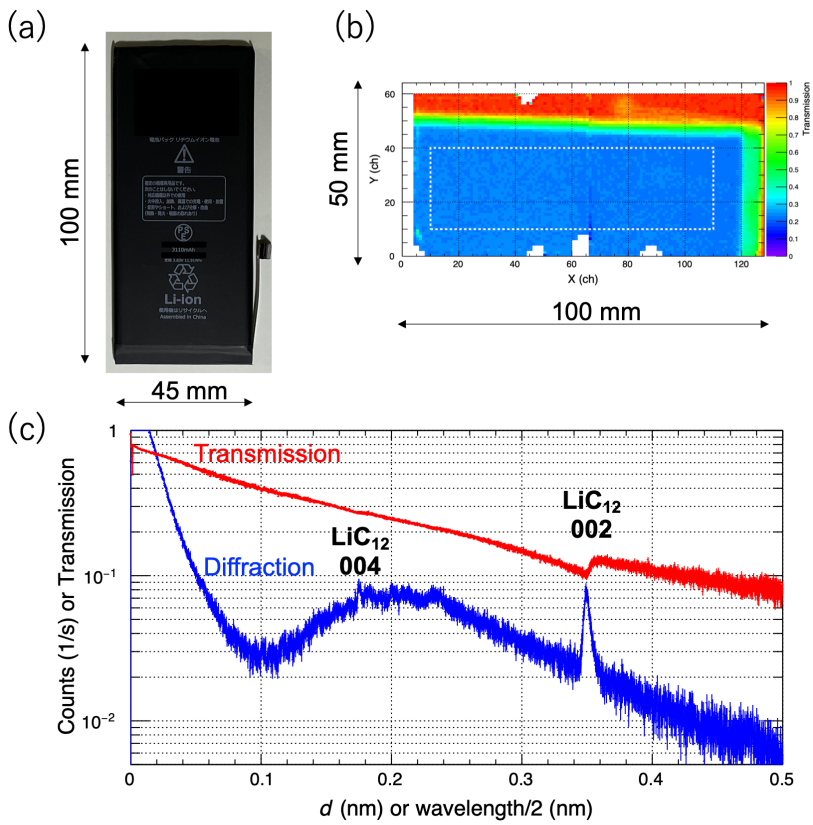

Fig. 3 Non-destructive analysis of a lithium-ion battery. (a) Photograph of the sample.
(b) Neutron transmission image with a wavelength range from 0.24 to 0.73 nm. (c) Diffraction and transmission spectra.

The measurement was performed using a Li-glass scintillation 2D detector, which can record the TOF data with the 2D spatial position information for each neutron. The spatial resolution of the detector is approximately 1 mm. The measurement times are 1 hour with the sample and without the sample. The latter measurement is necessary for obtaining neutron transmission of the sample.

Fig. 3 (b) is the transmission image with a wavelength range from 0.24 to 0.73 nm. The sample shape can be recognized. Fig. 3 (c) is the transmission spectrum, whose horizontal axis is a half of the neutron wavelength, obtained in the dashed-line area in Fig. 3(b). Additionally, a diffraction spectrum, whose horizontal axis is the lattice spacing, is overlapped. In the diffraction spectrum, the two clear peaks are recognized, and these are originating from the LiC_{12} crystal in the graphite negative electrode. In the transmission spectrum, there are the Bragg edges corresponding to them. This result indicates that the Bragg-edge imaging of LIBs is possible at AISTANS. The diffraction data is helpful for understanding the Bragg-edge spectrum.

6 Summary

AISTANS is providing thermal-cold pulsed neutron beams by using the approximately 1 kW electron beam. The first neutron beamline, which is optimized for Bragg-edge imaging, is operational. Additionally, a second beamline, which is designed to be used for neutron radiography, CT, and fast neutron irradiation, has just been constructed and will become operational soon. The neutron non-destructive analyses are performed with various methods of radiography, CT, Bragg-edge imaging, and diffraction. From the beginning of the AISTANS operation, various automobile samples have been analysed. Recently we are expanding the industrial applications to LIBs etc. and have succeeded in obtaining and understanding the Bragg-edge spectrum, which will become the basis for future Bragg-edge imaging.

References

1. K. Kino, M. Furusaka, T. Fujiwara, B.E. O'Rourke. T. Muroga, Y. Tomota, N. Oshima, Eur. Phys. J. Plus, **137**, 1260 (2022)
2. K. Kino *et al*., Nucl. Instrum. Methods Phys. Res., **A 927**, 407 (2019)
3. B.E. O'Rourke *et al*., Nucl. Instrum. Methods Phys. Res., **B 464**, 41 (2020)
4. T. Fujiwara *et al*., Rev. Sci. Instrum., **93**, 013304 (2022)
5. L.H. Schwartz, Nucl. Instrum. Methods, **42**, 81 (1966)
6. K. Kino *et al*., J. Neutron Res., **24**, 395 (2022)
7. K. Kino *et al*., Appl. Phys. Express, **15**, 027005 (2022)
8. T. Kamiyama, Y. Narita, H. Sato, M. Ohnuma, Y. Kiyanagi, Phys. Proc., **88**, 27 (2017)
9. K. Kino, M. Yonemura, Y. Ishikawa, T. Kamiyama, Solid State Ionics, **288**, 257 (2016)